

Received January 26, 2019, accepted February 19, 2019, date of publication February 22, 2019, date of current version March 12, 2019.

Digital Object Identifier 10.1109/ACCESS.2019.2901016

Design and Performance Analysis of Differential Chaos Shift Keying System With Dual-Index Modulation

XIANGMING CAI^{ID}, WEIKAI XU^{ID}, (Member, IEEE),

LIN WANG^{ID}, (Senior Member, IEEE),

AND FANG XU

School of Information Science and Engineering, Xiamen University, Xiamen 361005, China

Corresponding author: Weikai Xu (xweikai@xmu.edu.cn)

This work was supported by the National Natural Science Foundation of China under Grant 61671395 and Grant 61871337.

ABSTRACT In order to sufficiently utilize the time slot resources of the recently proposed pulse-position-modulation differential chaos shift keying (PPM-DCSK), we apply dual-index modulation to differential chaos shift keying and then present two differential chaos shift keying systems with dual-index modulation (DCSK-DIM), where the transmitted bits are partitioned into two orthogonal branches correspond to the in-phase branch and quadrature branch, respectively. Then, by means of the dual-index modulation technique, the mapped bits of in-phase and quadrature branches are modulated into a pair of distinguishable index symbols and thus recycle the time slot resources. At the receiver, two different detection methods are employed to determine the index symbols and demodulate the modulated bits carried by the active time slots. In addition, we derive the theoretical bit error rate (BER) expressions for the proposed DCSK-DIM systems over additive white Gaussian noise and multipath Rayleigh fading channels, respectively. In addition, then the simulation results validate the corresponding theoretical derivations. Finally, compared with other non-coherent chaotic communication systems, the proposed DCSK-DIM systems can achieve an excellent BER performance or data rate. Explicitly, the DCSK-DIM-I system makes a great progress in pursuit of admirable BER performance, while the DCSK-DIM-II system elevates the data rate to great extent.

INDEX TERMS Chaotic communication, differential chaos shift keying, dual-index modulation, bit error rate (BER).

I. INTRODUCTION

As a type of wideband, non-periodic and noise-like signals, chaotic signal can serve as an excellent candidate for spread-spectrum (SS) communication. In this vein, chaotic communication takes advantage of chaotic signals as carriers and exhibits great superiority, such as simple transceiver circuits, mitigation of fading in time varying channels [1], jamming resistance along with low probability of interception (LPI) [2] and secure communications [3]. As we well-known, depending on whether chaotic synchronization is required at the receiver terminal or not, the chaotic communication schemes can be divided into two categories, i.e., coherent and non-coherent schemes. The chaos shift keying (CSK) is a classical coherent scheme reported in [4]. Although many research

The associate editor coordinating the review of this manuscript and approving it for publication was Miaowen Wen.

buddies have made great efforts to explore the effective chaos-synchronization algorithms, unfortunately, those methods merely attained rather slow progress [5]–[8], which has severely hindered the further development of coherent chaotic communication schemes. Without the demand of complex chaotic synchronization and the channel state information at the receiver, non-coherent schemes have drawn a great deal of attention in the area of chaotic communication in the past few years.

Differential chaos shift keying (DCSK) [9] is the most popular non-coherent chaotic communication scheme, which has been studied extensively since it was born. Then, the DCSK scheme has stepped into a track of fast development and a mass of meritorious variants of DCSK have been proposed and analyzed by researches. Since the half of bit duration is spent sending non-information-bearing reference samples [10], the data rate and energy efficiency of DCSK

are rather low. To address this drawback, quadrature chaos shift keying (QCSK) [11] is proposed by Galias *et al.*, which is characterized by double data rate compared to DCSK, with the same bandwidth occupation. Moreover, the authors of [12] extend the QCSK (referred to as 4-ary DCSK) into M -ary DCSK and then propose a new multiresolution M -ary DCSK scheme which can provide different quality of services (QoS) according to their diverse levels of importance.

Another alternative method to elevate the data rate is multilevel modulation. In [13], a multilevel DCSK system is presented, which employs the orthogonality of Walsh code sequences to transmit more bits. Besides, two multilevel DCSK schemes, namely generalized code-shifted DCSK (GCS-DCSK) and its improved version multilevel code-shifted DCSK (MCS-DCSK), are reported in [14] and [15], respectively. Enjoying the excellent orthogonality of different chaotic sequences, a high-data-rate code-shifted DCSK (HCS-DCSK) is presented in [16], which can offer high data rate and strengthen data security. Recently, by using the orthogonal Walsh code sequences to carry the in-phase component and quadrature component of M -ary constellation symbol, Cai *et al.* [17] propose a multilevel code-shifted DCSK with M -ary modulation, which makes great progress in pursuit of high data rate and preferable BER performance.

Tremendous efforts have recently been spent on settling the issues related to minimizing the energy consumption and the complexity of communication systems while maximizing their data rate [18]. In this vein, index modulation (IM) was born under this background and IM techniques, which consider innovative ways to convey information compared to traditional communication systems, appear as competitive candidates for next generation wireless networks due to the attractive advantages they offer in terms of the spectral and energy efficiency as well as hardware simplicity [19]. In addition, IM systems can provide completely new dimensions for conveying data transmission by shifting the on/off status of different transmission entities including transmitting antennas, spreading codes, time slots and so on.

In the past few years, as a type of IM, code index modulation (CIM) was first introduced into direct sequence spread-spectrum (DSSS) system by Kaddoum *et al.* [20], [21]. In this design, the use of the spreading code index as an information bearing unit can promote the energy efficiency, enhance the overall spectral efficiency, reduce the hardware complexity and provide an excellent BER performance. Motivated by the above significant works, Xu *et al.* [22] make a powerful combination between GCS-DCSK system and CIM, and then propose a new non-coherent chaotic communication system named CIM-CS-DCSK, aiming at increasing the data rate in contrast to GCS-DCSK. Similarly, by combining MCS-DCSK system with CIM, Tan *et al.* [23] present a code index modulation multilevel code shifted DCSK referred to as CIM-MCS-DCSK. When appropriate parameters are considered, both the data rate and BER performance of CIM-MCS-DCSK system are superior to the counterparts of

MCS-DCSK system. More recently, a novel short reference DCSK (SR-DCSK) [24] with code index modulation called CIM-DCSK is reported in [25]. Besides, to further improve the BER performance of CIM-DCSK system, two additional optimization techniques have also been elaborated: the noise-reduction method [26] and the power-coefficient optimization algorithm [27].

Some research attempt has been devoted to investigating the chaotic-sequence-based index modulation. Recently, a new non-coherent commutation code index DCSK, i.e., CCI-DCSK, is presented in [28]. In this configuration, CCI-DCSK system exploits the benefits of IM by mapping extra bits into distinct commutated replicas of the reference chaotic sequence, which is then used for spreading a modulated bit. In a similar manner, permutation index DCSK namely PI-DCSK is proposed in [29] with the target of strengthening the data security, promoting the spectral efficiency and reducing the energy consumption. Besides, the idea of carrier index modulation has been introduced into the multi-carrier DCSK (MC-DCSK) [30], then the carrier index DCSK (CI-DCSK) [31] and its M -ary version (CI-MDCSK) [32] have been proposed to improve the BER performance and increase the data rate. In order to better recycle the subcarrier resources and gain higher spectral and energy efficiencies, a two-layer CI-DCSK (2CI-DCSK) has been reported in [33] and simulation results verify the advantages of this new design.

Lately, profiting from the pulse position modulation (PPM) and DCSK, Miao *et al.* [34] propose a hybrid modulation scheme, namely PPM-DCSK, to achieve preferable BER performance. Radically, PPM-DCSK system belongs to IM-based DCSK systems where the positions of different active time slots are served as a new dimension for data transmission. However, the BER performance improvement of PPM-DCSK system is at the expense of loss of spectrum resources, because the utilization of time slots is quite low which means a mass of inactive time slots do not convey any information bits. In order to settle this obstacle, we apply dual-index modulation to the conventional DCSK system and propose two novel differential chaos shift keying systems with dual-index modulation (DCSK-DIM) in this paper. The DCSK-DIM systems reuse all active time slots to implement dual-index modulation and then take full advantages of the superiority of dual-index modulation to elevate the data rate, spectral efficiency and BER performance to a great extent. The main contributions of this paper are summarized as follows:

- Two differential chaos shift keying systems with dual-index modulation are proposed, where the mapped bits corresponding to the in-phase and quadrature branches are modulated by a pair of distinguishable index symbols, respectively.
- In order to highlight the great advantage of the proposed systems with respect to the data rate, we make a comparison between DCSK-DIM systems and the recently proposed PPM-DCSK system. The comparison results

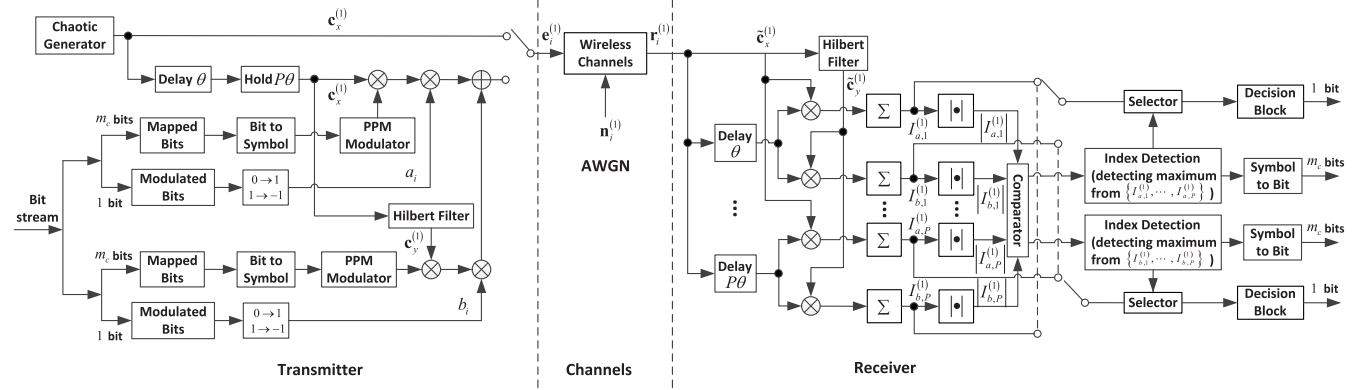


FIGURE 1. The block diagram of DCSK-DIM-I system.

demonstrate the DCSK-DIM systems possess higher data rate than its rival.

- The theoretical BER expressions of the DCSK-DIM systems are derived over additive white Gaussian noise and multipath Rayleigh fading channels, respectively. Subsequently, the simulation results validate the accuracy of our derivations.
- In contrast to the other non-coherent chaotic communication systems, the proposed two systems can achieve an excellent BER performance or data rate. Explicitly, the DCSK-DIM-I system makes a great progress in pursuit of admirable BER performance, while the DCSK-DIM-II system promotes the data rate to a great extent.

The remainder of this paper is organized as follows. The DCSK-DIM system models are described in Section II and the data rate, spectral efficiency comparisons and complexity analysis are provided in the same section. In Section III and IV, we derive the theoretical BER expressions for the DCSK-DIM-I and DCSK-DIM-II, respectively. Numerical results and discussions are given in Section V. Finally, Section VI concludes this paper.

II. DCSK-DIM SYSTEM

A. DCSK-DIM-I SYSTEM

The block diagram of DCSK-DIM-I system is depicted in Fig. 1. Clearly, there are two independent branches at the transmitter referred to as in-phase branch and quadrature branch, respectively. In each branch, the m_c bits are mapped into the index symbol to determine the active time slot of PPM signal and one bit is modulated into the active time slot for physically transmission. Subsequently, the signals from the in-phase and quadrature branches are overlaying in time domain to form the information bearing signal. For the convenience of readers' understanding, as shown in Fig. 2, we take a frame format as an example to elaborate how the information bearing signal is formed in DCSK-DIM-I system. In Case I, when the mapped bits of two branches are the same, the active time slots lie in the same location. As for Case II, the active slots of the two branches are different from

each other. Therefore, the transmitted signal $e_i^{(1)}$ is stated as

$$e_i^{(1)} = \left[\underbrace{c_x^{(1)}}_{\text{reference}}, \underbrace{S_{PPM}^{u_a} \otimes a_i c_x^{(1)} + S_{PPM}^{u_b} \otimes b_i c_y^{(1)}}_{\text{information - bearing}} \right], \quad (1)$$

where $c_x^{(1)}$ is a θ -length chaotic sequence and its orthogonal chaotic sequence is $c_y^{(1)}$ constructed by Hilbert filter, namely $c_y^{(1)} = \mathcal{H}(c_x^{(1)})$, where $\mathcal{H}(\cdot)$ denotes the Hilbert transform operation. $a_i, b_i \in \{-1, 1\}$ are the transmitted information symbols and \otimes represents Kronecker operator. Then, $S_{PPM}^{u_a} = [0, 0, \dots, 1_{u_a}, \dots, 0]_{1 \times P}$ ($P = 2^{m_c}$) is the PPM signal, where 1_{u_a} means that the u_a^{th} position of $S_{PPM}^{u_a}$ is equal to 1 which is determined by the mapped bits. $S_{PPM}^{u_b}$ can be represented in a similar manner. In this paper, we define the symbol duration of the proposed DCSK-DIM-I system as the spreading factor, namely $\beta = (P + 1)\theta$.

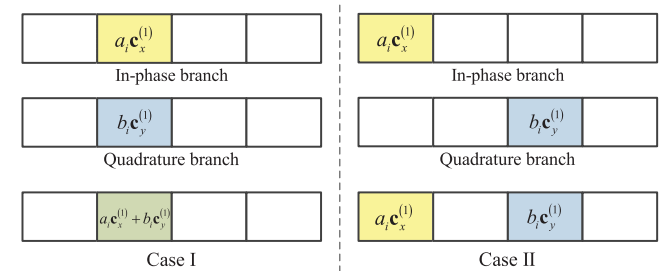


FIGURE 2. An example for the forming of information bearing signal in DCSK-DIM-I system.

Assuming that the transmitted signal $e_i^{(1)}$ is contaminated by the multipath fading and AWGN, the received signal $r_i^{(1)}$ can be formulated as

$$r_i^{(1)} = \sum_{l=1}^L \alpha_{i,l} e_{i-\tau_{i,l}}^{(1)} + n_i^{(1)}, \quad (2)$$

where L is the number of path, $\alpha_{i,l}$ and $\tau_{i,l}$ are the channel coefficient and the path delay of the l^{th} path, respectively. Then, $n_i^{(1)}$ denotes the wideband additive white Gaussian

noise vector with zero mean and covariance $\frac{N_0}{2}\mathbf{I}$, where \mathbf{I} is an identity matrix. Note that when the channel parameters satisfy $L = 1$, a unit channel coefficient $\alpha_{i,1} = 1$ and zero time delay $\tau_{i,1} = 0$, the channel degrades into the case of AWGN channel. For brevity, the subscript i will be omitted in the following analysis. As observed in Fig. 1, in order to retrieve the transmitted bits, the receiver not only needs to detect the modulated bits from the active time slots of in-phase and quadrature branches, but also the index symbols of PPM signals. In this vein, we first extract the reference signal $\tilde{\mathbf{c}}_x^{(1)}$ from the received signal $\mathbf{r}_i^{(1)}$. In addition, the reference signal $\tilde{\mathbf{c}}_x^{(1)}$ is loaded into the Hilbert filter to obtain its orthogonal signal $\tilde{\mathbf{c}}_y^{(1)}$, i.e., $\tilde{\mathbf{c}}_y^{(1)} = \mathcal{H}(\tilde{\mathbf{c}}_x^{(1)})$. Then, the signals $\tilde{\mathbf{c}}_x^{(1)}$ and $\tilde{\mathbf{c}}_y^{(1)}$ should be correlated with information bearing signal to obtain the decision variables $I_{a,p}^{(1)}$ and $I_{b,p}^{(1)}$, respectively, formulated as

$$I_{a,p}^{(1)} = \left[\tilde{\mathbf{c}}_x^{(1)} \right] \left[\mathbf{r}_{inf,p}^{(1)} \right]^T, \quad p = 1, 2, \dots, P, \quad (3)$$

$$I_{b,p}^{(1)} = \left[\tilde{\mathbf{c}}_y^{(1)} \right] \left[\mathbf{r}_{inf,p}^{(1)} \right]^T, \quad p = 1, 2, \dots, P. \quad (4)$$

where $\mathbf{r}_{inf,p}$, $p = 1, 2, \dots, P$ denotes the θ -length information bearing signal and $[\cdot]^T$ is transpose operator. Therefore, the two index symbols and their corresponding information symbols can be estimated by

$$\hat{u}_a^{(1)} = \arg \max_{p=1,2,\dots,P} \left(|I_{a,p}^{(1)}| \right), \quad (5)$$

$$\hat{u}_b^{(1)} = \arg \max_{p=1,2,\dots,P} \left(|I_{b,p}^{(1)}| \right), \quad (6)$$

$$\hat{a}_i^{(1)} = \text{sign} \left(I_{a,\hat{u}_a^{(1)}} \right), \quad (7)$$

$$\hat{b}_i^{(1)} = \text{sign} \left(I_{b,\hat{u}_b^{(1)}} \right). \quad (8)$$

Finally, the mapped bits as well as the modulated bits are recovered by converting the above symbols into binary bits.

B. DCSK-DIM-II SYSTEM

The block diagram of DCSK-DIM-II system is similar to that of DCSK-DIM-I system, thus the DCSK-DIM-II system model is omitted for the sake of brevity. In DCSK-DIM-II system, the number of the active time slots for each branch is $P - 1$ and the only one idle time slot is determined by the mapped bits differed from the DCSK-DIM-I system. Thus the total number of the transmitted bits within single DCSK-DIM-II symbol is equal to $2(m_c + P - 1)$. Similarly, an example for the forming of information bearing signal of DCSK-DIM-II system is illustrated in Fig. 3. Accordingly,

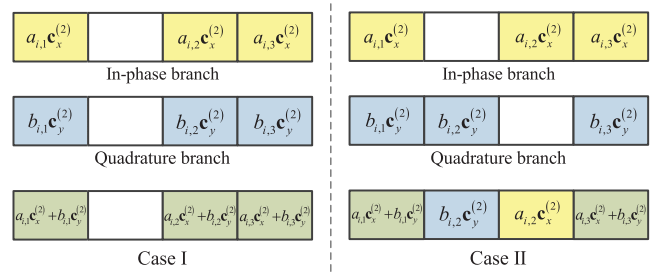


FIGURE 3. An example for the forming of information bearing signal in DCSK-DIM-II system.

the transmitted signal $\mathbf{e}_i^{(2)}$ can be represented by (9), as shown at the bottom of this page. In (9), $a_{i,m}, b_{i,n} \in \{-1, 1\}$ are the information symbols corresponding to m^{th} and n^{th} active time slots, respectively. Additionally, u_s and u_t denote the positions of idle time slots determined by the mapped bits of in-phase branch and quadrature branch, respectively. Apparently, the spreading factor of DCSK-DIM-II system is the same as that of DCSK-DIM-I system. When the transmitted signal $\mathbf{e}_i^{(2)}$ is polluted by multipath fading and AWGN, similarly, the received signal $\mathbf{r}_i^{(2)}$ can be expressed as

$$\mathbf{r}_i^{(2)} = \sum_{l=1}^L \alpha_{i,l} \mathbf{e}_{i-\tau_{i,l}}^{(2)} + \mathbf{n}_i^{(2)}, \quad (10)$$

where $\mathbf{n}_i^{(2)}$ denotes the AWGN with the same mean and covariance of $\mathbf{n}_i^{(1)}$. At the receiver, the reference signal and its corresponding orthogonal signal are obtained by a manipulation which is similar to DCSK-DIM-I system. In order to recover the mapped bits and modulated bits, the received reference signal and its orthogonal signal need to be correlated with each θ -length parts of information bearing signal, respectively. Then, different decision variables $I_{a,m}^{(2)}$, $m = 1, 2, \dots, P$ and $I_{b,n}^{(2)}$, $n = 1, 2, \dots, P$ are obtained. In order to determine the index symbols, we should make a comparison and find the subscripts corresponding to the minimum absolute values of decision variables, described as

$$\hat{u}_s = \arg \min_{m=1,2,\dots,P} \left(|I_{a,m}^{(2)}| \right), \quad (11)$$

$$\hat{u}_t = \arg \min_{n=1,2,\dots,P} \left(|I_{b,n}^{(2)}| \right). \quad (12)$$

According to the index symbols \hat{u}_s and \hat{u}_t , we can estimate the information symbols by

$$\hat{a}_m = \text{sign} \left(I_{a,m}^{(2)} \right), \quad m = 1, 2, \dots, P, m \neq \hat{u}_s, \quad (13)$$

$$\hat{b}_n = \text{sign} \left(I_{b,n}^{(2)} \right), \quad n = 1, 2, \dots, P, n \neq \hat{u}_t. \quad (14)$$

$$\mathbf{e}_i^{(2)} = \left[\underbrace{\mathbf{c}_x^{(2)} \text{ , reference}}_{\text{reference}} \underbrace{\sum_{m=1, m \neq u_s}^P \mathbf{S}_{PPM}^m \otimes a_{i,m} \mathbf{c}_x^{(2)} + \sum_{n=1, n \neq u_t}^P \mathbf{S}_{PPM}^n \otimes b_{i,n} \mathbf{c}_y^{(2)}}_{\text{information-bearing}} \right]. \quad (9)$$

Finally, after transforming the symbols above into binary bits, the mapped bits and the modulated bits can be retrieved in the output terminal.

C. DATA RATE AND SPECTRAL EFFICIENCY COMPARISONS

In this subsection, we make a comparison between the DCSK-DIM-I, DCSK-DIM-II and the recently proposed PPM-DCSK system with respect to the data rate and spectral efficiency. For a fair comparison, we define the total number of the transmitted bits within a symbol as the data rate R . Clearly, since the number of the active time slots for each branch is only one in DCSK-DIM-I system and this system possesses the advantages of dual-index modulation, the data rate of DCSK-DIM-I system is calculated as $R_I = 2(\log_2 P + 1)$. Unlike the case of DCSK-DIM-I system, in each branch, the DCSK-DIM-II system uses $P - 1$ active time slots to convey the information bits and the inactive time slot is merely one. In this vein, the data rate of the DCSK-DIM-II system can be formulated as $R_{II} = 2(\log_2 P + P - 1)$. Moreover, as for the PPM-DCSK system, its data rate can be given as $R_P = \log_2 P + 1$ [34].

TABLE 1. Data rate comparison between DCSK-DIM-I, DCSK-DIM-II and PPM-DCSK.

P	2	4	8	16	32	64
DCSK-DIM-I (R_I)	4	6	8	10	12	14
DCSK-DIM-II (R_{II})	4	10	20	38	72	138
PPM-DCSK (R_P)	2	3	4	5	6	7

The data rate comparison between the proposed DCSK-DIM-I, DCSK-DIM-II and the recently proposed PPM-DCSK system is shown in Table 1. It is worth noting that the DCSK-DIM-II system obtains the highest data rate than DCSK-DIM-I and PPM-DCSK systems, which is owing to that the number of the active time slots in DCSK-DIM-II system exceeds the two systems above. To be specific, the data rate of DCSK-DIM-I system is twice that of the recently proposed PPM-DCSK system, while the data rate of DCSK-DIM-II is more than five times that of PPM-DCSK system when $P > 8$. According to the above analysis and comparison, there is no dispute that the proposed DCSK-DIM-II system makes a great progress in pursuit of the high data rate.

Spectral efficiency is another imperative indicator to assess the system performance. Assuming that the bandwidth is equal to B in all the systems above, the spectral efficiency of the proposed DCSK-DIM-I system can be formulated as $SE_I = \frac{2(m_c+1)}{(1+2^m_c)\theta B}$. Similarly, the spectral efficiency of DCSK-DIM-II and PPM-DCSK systems can be expressed as $SE_{II} = \frac{2(m_c+2^m_c-1)}{(1+2^m_c)\theta B}$ and $SE_P = \frac{m_c+1}{(1+2^m_c)\theta B}$, respectively. Moreover, the spectral efficiency of PI-DCSK is given as $SE_{PI} = \frac{m_c+1}{2\theta B}$, while the counterpart of CCI-DCSK can be obtained as $SE_C = \frac{m_c+1}{\theta B}$. The comparisons of spectral efficiency between the proposed DCSK-DIM-I and DCSK-DIM-II systems and other state-of-the-art chaotic index modulation schemes are illustrated as the following Table 2.

TABLE 2. Spectral efficiency comparisons between DCSK-DIM-I, DCSK-DIM-II and other chaotic index modulation schemes.

Modulation Scheme	Spectral Efficiency
DCSK-DIM-I	$\frac{2(m_c+1)}{(1+2^m_c)\theta B}$
DCSK-DIM-II	$\frac{2(m_c+2^m_c-1)}{(1+2^m_c)\theta B}$
PPM-DCSK	$\frac{m_c+1}{(1+2^m_c)\theta B}$
PI-DCSK	$\frac{m_c+1}{2\theta B}$
CCI-DCSK	$\frac{m_c+1}{\theta B}$

As tabulated in Table 2, since the proposed DCSK-DIM-I and DCSK-DIM-II systems take full advantages of the time slot resource, the DCSK-DIM-I and DCSK-DIM-II systems can obtain higher spectral efficiency than PPM-DCSK system. Unfortunately, in contrast to PI-DCSK and CCI-DCSK systems, the spectral efficiency of DCSK-DIM-I and DCSK-DIM-II systems suffer sharp reduction with the reason of long symbol duration.

D. COMPLEXITY ANALYSIS AND COMPARISON

In this subsection, the hardware complexity of the proposed DCSK-DIM-I and DCSK-DIM-II systems are compared to the counterpart of PPM-DCSK system with the same parameter P , as they share similar modulation properties. Table 3 and Table 4 display the elements of transmitters and receivers towards the three systems above, respectively. In order to realize the dual-index modulation, the proposed DCSK-DIM-I and DCSK-DIM-II systems introduce the Hilbert filter in both transmitters and receivers which makes DCSK-DIM-I and DCSK-DIM-II system slightly difficult to be implemented. Whereas, the obtained benefit of the DCSK-DIM-I and DCSK-DIM-II systems is a tremendous advance in the aspect of data rate improvement. Furthermore, with respect to DCSK-DIM-II system, since more time slots are active which means higher data rate is available, the element number of adders, multipliers and PPM modulators is several times that of DCSK-DIM-I system.

TABLE 3. Transmitter hardware complexity comparisons between DCSK-DIM-I, DCSK-DIM-II and PPM-DCSK.

Elements	DCSK-DIM-I	DCSK-DIM-II	PPM-DCSK
Delay units	P	P	P
Adders	1	$2P - 3$	0
Multipliers	4	$4(P - 1)$	2
Hilbert filters	1	1	0
PPM modulators	2	$2(P - 1)$	1

TABLE 4. Receiver hardware complexity comparisons between DCSK-DIM-I, DCSK-DIM-II and PPM-DCSK.

Elements	DCSK-DIM-I	DCSK-DIM-II	PPM-DCSK
Delay units	P	P	P
Multipliers	$2P$	$2P$	P
Hilbert filters	1	1	0
Index detection	2	2	1

III. PERFORMANCE ANALYSIS OF DCSK-DIM-I SYSTEM

Since the dual-index modulation is applied to the DCSK-DIM-I system, the active time slots corresponding to

in-phase and quadrature branches are independent of each other. As shown in Fig. 2, there are two different cases to consider, according to whether the two index symbols in dual-index modulation are the same or not, in the following analysis.

1) Case I: The index symbols are the same, which means that the positions of the active time slots are identical.

2) Case II: The index symbols differ from each other, which represents that the active time slots are in different locations.

A. CASE I: THE SAME INDEX SYMBOLS

In this case, since the index symbols of the in-phase and quadrature branches are the same and have the identical error probability, we only need to evaluate the error performance of one of them. When the index detection of in-phase branch is correct, i.e., $p = \hat{u}_a$, the decision variable $I_{a,\hat{u}_a}^{(1)}$ is given as

$$I_{a,\hat{u}_a}^{(1)} = \left(\sum_{l=1}^L \alpha_l \mathbf{c}_{x,\tau_l}^{(1)} + \mathbf{n}_r^{(1)} \right) \times \left(\sum_{l=1}^L \alpha_l \left(a_i \mathbf{c}_{x,\tau_l}^{(1)} + b_i \mathbf{c}_{y,\tau_l}^{(1)} \right) + \mathbf{n}_{inf,\hat{u}_a}^{(1)} \right)^T, \quad (15)$$

where $\mathbf{n}_r^{(1)}$ and $\mathbf{n}_{inf,\hat{u}_a}^{(1)}$ are the AWGN with the same means and covariances of $\mathbf{n}_i^{(1)}$. Moreover, $\mathbf{c}_{x,\tau_l}^{(1)}$ and $\mathbf{c}_{y,\tau_l}^{(1)}$ denote the delayed reference sequence and its orthogonal sequence, respectively. As a result, the mean and variance of $I_{a,\hat{u}_a}^{(1)}$ are calculated as

$$\begin{aligned} \mathbb{E}[I_{a,\hat{u}_a}^{(1)}] &= \sum_{l=1}^L \alpha_l^2 \theta \mathbb{E}[c_I^2] = \sum_{l=1}^L \alpha_l^2 \frac{E_s^{(1)}}{3} \\ &= \sqrt{\sum_{l=1}^L \alpha_l^2 E_s^{(1)} N_0} \underbrace{\left(\frac{\sqrt{\gamma_s^{(1)}}}{3} \right)}_{\Delta} = \mu_1, \end{aligned} \quad (16)$$

$$\begin{aligned} \text{Var}[I_{a,\hat{u}_a}^{(1)}] &= \sum_{l=1}^L \alpha_l^2 3\theta \mathbb{E}[c_I^2] \frac{N_0}{2} + \theta \frac{N_0^2}{4} \\ &= \sum_{l=1}^L \alpha_l^2 \frac{E_s^{(1)} N_0}{2} + \theta \frac{N_0^2}{4} \\ &= \sum_{l=1}^L \alpha_l^2 E_s^{(1)} N_0 \underbrace{\left(\frac{1}{2} + \frac{\theta}{4\gamma_s^{(1)}} \right)}_{\kappa} = \sigma_1^2, \end{aligned} \quad (17)$$

where $\mathbb{E}[\cdot]$ and $\text{Var}[\cdot]$ are the mean operator and variance operator, respectively. $E_s^{(1)}$ is the symbol energy of DCSK-DIM-I, given as $E_s^{(1)} = 3\theta \mathbb{E}[c_I^2]$ and $\mathbb{E}[c_I^2] = \mathbb{E}\left[\left(\mathbf{c}_{x,\tau_l}^{(1)}\right)^2\right] = \mathbb{E}\left[\left(\mathbf{c}_{y,\tau_l}^{(1)}\right)^2\right]$ is the chip energy. Besides, $\gamma_s^{(1)}$ is the symbol signal-to-noise ratio (SNR), given as $\gamma_s^{(1)} = \sum_{l=1}^L \alpha_l^2 \frac{E_s^{(1)}}{N_0}$. When the index detection is incorrect,

namely $p \neq \hat{u}_a$, the decision variable $I_{a,p}^{(1)}$ can be stated as

$$I_{a,p}^{(1)} = \left(\sum_{l=1}^L \alpha_l \mathbf{c}_{x,\tau_l}^{(1)} + \mathbf{n}_r^{(1)} \right) \left(\mathbf{n}_{inf,p}^{(1)} \right)^T. \quad (18)$$

Therefore, the mean and variance of $I_{a,p}^{(1)}$ are obtained as

$$\mathbb{E}[I_{a,p}^{(1)}] = 0 = \mu_2, \quad (19)$$

$$\text{Var}[I_{a,p}^{(1)}] = \sum_{l=1}^L \alpha_l^2 E_s^{(1)} N_0 \underbrace{\left(\frac{1}{6} + \frac{\theta}{4\gamma_s^{(1)}} \right)}_{\Omega} = \sigma_2^2. \quad (20)$$

When the absolute value of $I_{a,\hat{u}_a}^{(1)}$ corresponding to the correct index detection is less than the counterpart of $I_{a,p}^{(1)}$ corresponding to the incorrect index detection, an error will occur. Hence, the erroneous index detection probability in Case I is formulated by [29]

$$\begin{aligned} P_{ed,I}^{(1)} &= 1 - \Pr\left[|I_{a,\hat{u}_a}^{(1)}| > \max(|I_{a,p}^{(1)}|)\right] \\ &= 1 - \int_0^\infty \left(F_{|I_{a,p}^{(1)}|}(x, \mu_2, \sigma_2^2) \right)^{P-1} \\ &\quad \times f_{|I_{a,\hat{u}_a}^{(1)}|}(x, \mu_1, \sigma_1^2) dx, \end{aligned} \quad (21)$$

where $F_{|I_{a,p}^{(1)}|}(x, \mu_2, \sigma_2^2)$ is the cumulative distribution function of $|I_{a,p}^{(1)}|$ and $f_{|I_{a,\hat{u}_a}^{(1)}|}(x, \mu_1, \sigma_1^2)$ denotes the probability density function of $|I_{a,\hat{u}_a}^{(1)}|$. To be specific, $F_{|I_{a,p}^{(1)}|}(x, \mu_2, \sigma_2^2)$ and $f_{|I_{a,\hat{u}_a}^{(1)}|}(x, \mu_1, \sigma_1^2)$ can be represented in a general form as [35]

$$F_{|I|}(x, \mu, \sigma^2) \equiv \frac{1}{2} \left[\operatorname{erf}\left(\frac{x-\mu}{\sqrt{2\sigma^2}}\right) + \operatorname{erf}\left(\frac{x+\mu}{\sqrt{2\sigma^2}}\right) \right], \quad (22)$$

$$f_{|I|}(x, \mu, \sigma^2) \equiv \frac{1}{\sqrt{2\pi\sigma^2}} \left(e^{-\frac{(x-\mu)^2}{2\sigma^2}} + e^{-\frac{(x+\mu)^2}{2\sigma^2}} \right), \quad (23)$$

where $\operatorname{erf}(x) = \frac{2}{\sqrt{\pi}} \int_0^x e^{-t^2} dt$ represents the well-known error function. Then, substituting $x = \sqrt{\sum_{l=1}^L \alpha_l^2 E_s^{(1)} N_0 \xi}$ and $d\xi = \sqrt{\sum_{l=1}^L \alpha_l^2 E_s^{(1)} N_0} d\xi$ into (21), the erroneous index detection probability $P_{ed,I}^{(1)}$ can be further simplified as

$$\begin{aligned} P_{ed,I}^{(1)} &= 1 - \frac{1}{\sqrt{2\pi\kappa}} \int_0^\infty \left[\operatorname{erf}\left(\frac{\xi}{\sqrt{2\Omega}}\right) \right]^{P-1} \\ &\quad \times \left(e^{-\frac{(\xi-\Delta)^2}{2\kappa}} + e^{-\frac{(\xi+\Delta)^2}{2\kappa}} \right) d\xi. \end{aligned} \quad (24)$$

Hence, the bit error probability of the mapped bits is obtained as [29] and [36]

$$P_{map,I}^{(1)} = \frac{2^{(m_c-1)}}{2^{m_c}-1} P_{ed,I}^{(1)} \equiv g(m_c, P_{ed,I}^{(1)}). \quad (25)$$

Furthermore, the bit error rate of the modulated bits is represented as [21]

$$P_{mod,I}^{(1)} = P_{e,I}^{(1)} \left(1 - P_{ed,I}^{(1)} \right) + \frac{1}{2} P_{ed,I}^{(1)}. \quad (26)$$

In (26), $P_{e,I}^{(1)} = \frac{1}{2} \operatorname{erfc} \left[\left(\frac{2\sigma_1^2}{\mu_1^2} \right)^{-\frac{1}{2}} \right]$, where $\operatorname{erfc}(x) = 1 - \operatorname{erf}(x)$ is the complementary error function. Finally, the BER of DCSK-DIM-I system in Case I is described as [28] and [29]

$$\begin{aligned} P_{sys,I}^{(1)} &= \frac{m_c}{m_c + 1} P_{map,I}^{(1)} + \frac{1}{m_c + 1} P_{mod,I}^{(1)} \\ &\equiv h(m_c, P_{map,I}^{(1)}, P_{mod,I}^{(1)}). \end{aligned} \quad (27)$$

B. CASE II: THE DIFFERENT INDEX SYMBOLS

In this case, the index symbols of in-phase and quadrature branch are different, thus the positions of the two active time slots are disparate and independent of each other. Generally, we make an assumption that the v^{th} and w^{th} ($w \neq v$) time slots corresponding to the in-phase branch and quadrature branch are active, respectively. When the index detection of the in-phase branch is correct, namely $p = v$, the decision variable $I_{a,v}^{(1)}$ is formulated as

$$I_{a,v}^{(1)} = \left(\sum_{l=1}^L \alpha_l \mathbf{c}_{x,\tau_l}^{(1)} + \mathbf{n}_r^{(1)} \right) \left(\sum_{l=1}^L \alpha_l a_l \mathbf{c}_{x,\tau_l}^{(1)} + \mathbf{n}_{inf,v}^{(1)} \right)^T. \quad (28)$$

As a result, the mean and variance of decision variable $I_{a,v}^{(1)}$ are calculated as

$$\mathbb{E}[I_{a,v}^{(1)}] = \sqrt{\sum_{l=1}^L \alpha_l^2 E_s^{(1)} N_0} \underbrace{\left(\frac{\sqrt{\gamma_s^{(1)}}}{3} \right)}_{\Delta} = \mu_1, \quad (29)$$

$$\operatorname{Var}[I_{a,v}^{(1)}] = \sum_{l=1}^L \alpha_l^2 E_s^{(1)} N_0 \underbrace{\left(\frac{1}{3} + \frac{\theta}{4\gamma_s^{(1)}} \right)}_{\chi} = \sigma_3^2. \quad (30)$$

Unlike the Case I, there are two different situations resulting in the error index detection of the in-phase branch. In the first situation, i.e., $p = w$, the decision variable $I_{a,w}^{(1)}$ can be represented by

$$I_{a,w}^{(1)} = \left(\sum_{l=1}^L \alpha_l \mathbf{c}_{x,\tau_l}^{(1)} + \mathbf{n}_r^{(1)} \right) \left(\sum_{l=1}^L \alpha_l b_l \mathbf{c}_{y,\tau_l}^{(1)} + \mathbf{n}_{inf,w}^{(1)} \right)^T. \quad (31)$$

In this vein, the mean and variance of $I_{a,w}^{(1)}$ are given as

$$\mathbb{E}[I_{a,w}^{(1)}] = 0 = \mu_2, \quad (32)$$

$$\operatorname{Var}[I_{a,w}^{(1)}] = \sum_{l=1}^L \alpha_l^2 E_s^{(1)} N_0 \underbrace{\left(\frac{1}{3} + \frac{\theta}{4\gamma_s^{(1)}} \right)}_{\chi} = \sigma_3^2. \quad (33)$$

Regarding the second situation, namely $p \neq v$ and $p \neq w$, the decision variable $I_{a,p}^{(1)}$ is stated as

$$I_{a,p}^{(1)} = \left(\sum_{l=1}^L \alpha_l \mathbf{c}_{x,\tau_l}^{(1)} + \mathbf{n}_r^{(1)} \right) \left(\mathbf{n}_{inf,p}^{(1)} \right)^T. \quad (34)$$

Thus, the mean and variance of $I_{a,p}^{(1)}$ are equal to

$$\mathbb{E}[I_{a,p}^{(1)}] = 0 = \mu_2, \quad (35)$$

$$\operatorname{Var}[I_{a,p}^{(1)}] = \sum_{l=1}^L \alpha_l^2 E_s^{(1)} N_0 \underbrace{\left(\frac{1}{6} + \frac{\theta}{4\gamma_s^{(1)}} \right)}_{\Omega} = \sigma_2^2. \quad (36)$$

When the absolute value of $I_{a,v}^{(1)}$ is less than the counterpart of $I_{a,p}^{(1)}$ and $I_{a,w}^{(1)}$, the index symbol of the in-phase branch is detected incorrectly. Hence, the erroneous index detection probability in Case II is formulated as

$$\begin{aligned} P_{ed,II}^{(1)} &= 1 - \Pr \left[|I_{a,v}^{(1)}| > \max \left(|I_{a,p}^{(1)}|, |I_{a,w}^{(1)}| \right) \right] \\ &= 1 - \int_0^\infty \left(F_{|I_{a,p}^{(1)}|} (x, \mu_2, \sigma_2^2) \right)^{P-2} \\ &\quad \times F_{|I_{a,w}^{(1)}|} (x, \mu_2, \sigma_3^2) f_{|I_{a,v}^{(1)}|} (x, \mu_1, \sigma_1^2) dx, \end{aligned} \quad (37)$$

After the similar manipulation as the Case I, the simplified erroneous index detection probability $P_{ed,II}^{(1)}$ is rewritten as

$$\begin{aligned} P_{ed,II}^{(1)} &= 1 - \frac{1}{\sqrt{2\pi}\chi} \int_0^\infty \left[\operatorname{erf} \left(\frac{\xi}{\sqrt{2\Omega}} \right) \right]^{P-2} \\ &\quad \times \left[\operatorname{erf} \left(\frac{\xi}{\sqrt{2\chi}} \right) \right] \left(e^{-\frac{(\xi-\Delta)^2}{2\chi}} + e^{-\frac{(\xi+\Delta)^2}{2\chi}} \right) d\xi. \end{aligned} \quad (38)$$

As a consequence, the bit error probability of the mapped bits and modulated bits are obtained, respectively, as

$$P_{map,II}^{(1)} = g(m_c, P_{ed,II}^{(1)}), \quad (39)$$

$$P_{mod,II}^{(1)} = P_{e,II}^{(1)} \left(1 - P_{ed,II}^{(1)} \right) + \frac{1}{2} P_{ed,II}^{(1)}, \quad (40)$$

where $P_{e,II}^{(1)} = \frac{1}{2} \operatorname{erfc} \left[\left(\frac{2\sigma_3^2}{\mu_1^2} \right)^{-\frac{1}{2}} \right]$. Finally, the BER of DCSK-DIM-I system in Case II is calculated as

$$P_{sys,II}^{(1)} = h(m_c, P_{map,II}^{(1)}, P_{mod,II}^{(1)}). \quad (41)$$

Assuming that the transmitted information bits are equiprobable, then the total bit error probability of the DCSK-DIM-I system is formulated as

$$P_{sys}^{(1)} = \frac{1}{P} P_{sys,I}^{(1)} + \frac{P-1}{P} P_{sys,II}^{(1)}. \quad (42)$$

According to [12] and [36], when the case of L independent and identically distributed (i.i.d) Rayleigh-fading channels are considered, the average bit error rate of DCSK-DIM-I system over multipath Rayleigh fading channel is stated as

$$\bar{P}_{sys}^{(1)} = \int_0^\infty P_{sys}^{(1)} f(\gamma_s^{(1)}) d\gamma_s^{(1)}, \quad (43)$$

where

$$f\left(\gamma_s^{(1)}\right) = \frac{\left(\gamma_s^{(1)}\right)^{L-1}}{(L-1)!\bar{\gamma}_c^L} \exp\left(-\frac{\gamma_s^{(1)}}{\bar{\gamma}_c}\right), \quad (44)$$

where $\bar{\gamma}_c = \frac{E_s^{(1)}}{N_0} E[\alpha_j^2] = \frac{E_s^{(1)}}{N_0} E[\alpha_l^2]$, $j \neq l$ is the average symbol-SNR per channel and $\sum_{l=1}^L E[\alpha_l^2] = 1$.

IV. PERFORMANCE ANALYSIS OF DCSK-DIM-II SYSTEM

As shown in Fig. 3, according to whether the index symbols corresponding to the in-phase and quadrature branches are the same or not, we will analyse the BER performance of the DCSK-DIM-II system from the following two cases:

1) Case I: The index symbols are alike to each other, i.e., the positions of the inactive time slots are identical.

2) Case II: The index symbols differ from each other, namely, the positions of the inactive time slots are disparate.

A. CASE I: THE SAME INDEX SYMBOLS

It is clearly observed that the index symbols of the in-phase and quadrature branches are independent of each other and the $P-1$ time slots of each branch are also independent, thus we merely need to evaluate the error performance of one of them. In this vein, when the index symbol corresponding to the in-phase branch is detected correctly, namely $m = \hat{u}_s$, the decision variable $I_{a,\hat{u}_s}^{(2)}$ is expressed as

$$I_{a,\hat{u}_s}^{(2)} = \left(\sum_{l=1}^L \alpha_l \mathbf{c}_{x,\tau_l}^{(2)} + \mathbf{n}_r^{(2)} \right) \left(\mathbf{n}_{inf,\hat{u}_s}^{(2)} \right)^T. \quad (45)$$

Therefore, the mean and variance of $I_{a,\hat{u}_s}^{(2)}$ are calculated as

$$E\left[I_{a,\hat{u}_s}^{(2)}\right] = 0 = \mu_2, \quad (46)$$

$$\begin{aligned} \text{Var}\left[I_{a,\hat{u}_s}^{(2)}\right] &= \sum_{l=1}^L \alpha_l^2 \theta E\left[c_{II}^2\right] \frac{N_0}{2} + \theta \frac{N_0^2}{4} \\ &= \sum_{l=1}^L \alpha_l^2 \frac{E_s^{(2)} N_0}{2(2P-1)} + \theta \frac{N_0^2}{4} \\ &= \sum_{l=1}^L \alpha_l^2 E_s^{(2)} N_0 \underbrace{\left(\frac{1}{2(2P-1)} + \frac{\theta}{4\gamma_s^{(2)}} \right)}_{\omega} = \sigma_4^2, \end{aligned} \quad (47)$$

where $E_s^{(2)} = (2P-1)\theta E\left[c_{II}^2\right]$ is the symbol energy of DCSK-DIM-II and $E\left[c_{II}^2\right] = E\left[\left(c_{x,\tau_l}^{(2)}\right)^2\right] = E\left[\left(c_{y,\tau_l}^{(2)}\right)^2\right]$ is the chip energy. When the index detection is incorrect, i.e., $m \neq \hat{u}_s$, the decision variable $I_{a,m}^{(2)}$ is given as

$$\begin{aligned} I_{a,m}^{(2)} &= \left(\sum_{l=1}^L \alpha_l \mathbf{c}_{x,\tau_l}^{(2)} + \mathbf{n}_r^{(2)} \right) \\ &\times \left(\sum_{l=1}^L \alpha_l \left(a_{i,m} \mathbf{c}_{x,\tau_l}^{(2)} + b_{i,n} \mathbf{c}_{y,\tau_l}^{(2)} \right) + \mathbf{n}_{inf,m}^{(2)} \right)^T. \end{aligned} \quad (48)$$

Similarly, the mean and variance of $I_{a,m}^{(2)}$ are obtained as

$$E\left[I_{a,m}^{(2)}\right] = \sqrt{\sum_{l=1}^L \alpha_l^2 E_s^{(2)} N_0} \underbrace{\left(\frac{\sqrt{\gamma_s^{(2)}}}{2P-1} \right)}_{\phi} = \mu_3, \quad (49)$$

$$\text{Var}\left[I_{a,m}^{(2)}\right] = \sum_{l=1}^L \alpha_l^2 E_s^{(2)} N_0 \underbrace{\left(\frac{3}{2(2P-1)} + \frac{\theta}{4\gamma_s^{(2)}} \right)}_{\rho} = \sigma_5^2. \quad (50)$$

When the absolute value of $I_{a,\hat{u}_s}^{(2)}$ is greater than the minimum of $I_{a,m}^{(2)}$, there will be an error in index detection. In this vein, the erroneous index detection probability for the Case I is represented as

$$\begin{aligned} P_{ed,I}^{(2)} &= \Pr\left[|I_{a,\hat{u}_s}^{(2)}| > \min(|I_{a,m}^{(2)}|)\right] \\ &= \int_0^\infty \left[1 - \left(1 - F_{|I_{a,m}^{(2)}|}(x, \mu_3, \sigma_5^2) \right)^{P-1} \right] \\ &\quad \times f_{|I_{a,\hat{u}_s}^{(2)}|}(x, \mu_2, \sigma_4^2) dx, \end{aligned} \quad (51)$$

Similar to the manipulation of DCSK-DIM-I system, the error probability $P_{ed,I}^{(2)}$ can be simplified as

$$\begin{aligned} P_{ed,I}^{(2)} &= \frac{2}{\sqrt{2\pi\omega}} \int_0^\infty \left[1 - \left(\frac{1}{2} \right)^{P-1} \left[\text{erfc}\left(\frac{x-\phi}{\sqrt{2\rho}}\right) \right. \right. \\ &\quad \left. \left. + \text{erfc}\left(\frac{x+\phi}{\sqrt{2\rho}}\right) \right]^{P-1} \right] e^{-\left(\frac{x^2}{2\omega}\right)} d\xi. \end{aligned} \quad (52)$$

Thus the BER of the mapped bits and the modulated bits are formulated, respectively, as

$$P_{map,I}^{(2)} = g(m_c, P_{ed,I}^{(2)}), \quad (53)$$

$$P_{mod,I}^{(2)} = P_{e,I}^{(2)} \left(1 - P_{ed,I}^{(2)} \right) + P_{n,I} \cdot P_{ed,I}^{(2)}, \quad (54)$$

where $P_{e,I}^{(2)} = \frac{1}{2} \text{erfc}\left[\left(\frac{2\sigma_5^2}{\mu_3^2}\right)^{-\frac{1}{2}}\right]$ and $P_{n,I} = \frac{0.5+(P-2)P_{e,I}^{(2)}}{P-1}$.

Finally, the bit error probability of DCSK-DIM-II system in Case I is written as

$$\begin{aligned} P_{sys,I}^{(2)} &= \frac{m_c}{m_c + 2^{m_c} - 1} P_{map,I}^{(2)} + \frac{2^{m_c} - 1}{m_c + 2^{m_c} - 1} P_{mod,I}^{(2)} \\ &\equiv \psi(m_c, P_{map,I}^{(2)}, P_{mod,I}^{(2)}). \end{aligned} \quad (55)$$

B. CASE II: THE DIFFERENT INDEX SYMBOLS

Without loss of generality, in this case, the j^{th} time slot corresponding to the in-phase branch is inactive, while the k^{th} time slots corresponding to the quadrature branch is inactive. Since the detection for the index symbols of in-phase and quadrature branches are independent of each other and have the same error probability, we analyse the detection of the in-phase branch for brevity. When the index symbol is

detected correctly, i.e., $m = j$, the decision variable $I_{a,j}^{(2)}$ is stated by

$$I_{a,j}^{(2)} = \left(\sum_{l=1}^L \alpha_l \mathbf{c}_{x,\tau_l}^{(2)} + \mathbf{n}_r^{(2)} \right) \left(\sum_{l=1}^L \alpha_l b_{i,n} \mathbf{c}_{y,\tau_l}^{(2)} + \mathbf{n}_{inf,j}^{(2)} \right)^T. \quad (56)$$

The mean and variance of $I_{a,j}^{(2)}$ can be calculated as

$$\mathbb{E}[I_{a,j}^{(2)}] = 0 = \mu_2, \quad (57)$$

$$\text{Var}[I_{a,j}^{(2)}] = \sum_{l=1}^L \alpha_l^2 E_s^{(2)} N_0 \underbrace{\left(\frac{1}{2P-1} + \frac{\theta}{4\gamma_s^{(2)}} \right)}_{v} = \sigma_6^2. \quad (58)$$

There are two situations resulting in the incorrect index detection of in-phase branch. As for the first situation, namely $m = k$, the decision variable $I_{a,k}^{(2)}$ is given as

$$I_{a,k}^{(2)} = \left(\sum_{l=1}^L \alpha_l \mathbf{c}_{x,\tau_l}^{(2)} + \mathbf{n}_r^{(2)} \right) \left(\sum_{l=1}^L \alpha_l a_{i,m} \mathbf{c}_{x,\tau_l}^{(2)} + \mathbf{n}_{inf,k}^{(2)} \right)^T. \quad (59)$$

Hence, the mean and variance of decision variable $I_{a,k}^{(2)}$ are formulated as

$$\mathbb{E}[I_{a,k}^{(2)}] = \sqrt{\sum_{l=1}^L \alpha_l^2 E_s^{(2)} N_0} \underbrace{\left(\frac{\sqrt{\gamma_s^{(2)}}}{2P-1} \right)}_{\phi} = \mu_3, \quad (60)$$

$$\text{Var}[I_{a,k}^{(2)}] = \sum_{l=1}^L \alpha_l^2 E_s^{(2)} N_0 \underbrace{\left(\frac{1}{2P-1} + \frac{\theta}{4\gamma_s^{(2)}} \right)}_{v} = \sigma_6^2. \quad (61)$$

With respect to the second situation, i.e., $m \neq j$ and $m \neq k$, the decision variable $I_{a,m}^{(2)}$ is represented as

$$I_{a,m}^{(2)} = \left(\sum_{l=1}^L \alpha_l \mathbf{c}_{x,\tau_l}^{(2)} + \mathbf{n}_r^{(2)} \right) \times \left(\sum_{l=1}^L \alpha_l \left(a_{i,m} \mathbf{c}_{x,\tau_l}^{(2)} + b_{i,n} \mathbf{c}_{y,\tau_l}^{(2)} \right) + \mathbf{n}_{inf,m}^{(2)} \right)^T. \quad (62)$$

As a result, the mean and variance of $I_{a,m}^{(2)}$ are expressed as

$$\mathbb{E}[I_{a,m}^{(2)}] = \sqrt{\sum_{l=1}^L \alpha_l^2 E_s^{(2)} N_0} \underbrace{\left(\frac{\sqrt{\gamma_s^{(2)}}}{2P-1} \right)}_{\phi} = \mu_3, \quad (63)$$

$$\text{Var}[I_{a,m}^{(2)}] = \sum_{l=1}^L \alpha_l^2 E_s^{(2)} N_0 \underbrace{\left(\frac{3}{2(2P-1)} + \frac{\theta}{4\gamma_s^{(2)}} \right)}_{\rho} = \sigma_5^2. \quad (64)$$

When the absolute value of decision variable $I_{a,j}^{(2)}$ is greater than the minimums of $I_{a,k}^{(2)}$ and $I_{a,m}^{(2)}$, an error will appear in index detection. As a consequence, the erroneous index detection probability in Case II can be formulated as

$$\begin{aligned} P_{ed,II}^{(2)} &= \Pr \left[|I_{a,j}^{(2)}| > \min \left(|I_{a,m}^{(2)}|, |I_{a,k}^{(2)}| \right) \right] \\ &= \int_0^\infty \left[1 - \left(1 - F_{|I_{a,m}^{(2)}|} (x, \mu_3, \sigma_5^2) \right) \right]^{P-2} \\ &\quad \times \left(1 - F_{|I_{a,k}^{(2)}|} (x, \mu_3, \sigma_6^2) \right) f_{|I_{a,j}^{(2)}|} (x, \mu_2, \sigma_6^2) dx. \end{aligned} \quad (65)$$

Let $x = \sqrt{\sum_{l=1}^L \alpha_l^2 E_s^{(2)} N_0 \xi}$ and $dx = \sqrt{\sum_{l=1}^L \alpha_l^2 E_s^{(2)} N_0} d\xi$ and then substituting them into (65), the erroneous index detection probability $P_{ed,II}^{(2)}$ can be simplified as (66), shown at the bottom of this page. Therefore, the bit error probability of the mapped bits and the modulated bits can be given as

$$P_{map,II}^{(2)} = g(m_c, P_{ed,II}^{(2)}), \quad (67)$$

$$P_{mod,II}^{(2)} = P_{e,II}^{(2)} \left(1 - P_{ed,II}^{(2)} \right) + P_{n,II} \cdot P_{ed,II}^{(2)}. \quad (68)$$

In (68), $P_{e,II}^{(2)} = \frac{P_k + (P-2)P_m}{P-1}$ and $P_{n,II} \approx \frac{0.5 + (P-2)P_m}{P-1}$, where

$$P_k = \frac{1}{2} \operatorname{erfc} \left[\left(\frac{2\sigma_6^2}{\mu_3^2} \right)^{-\frac{1}{2}} \right], \quad (69)$$

$$P_m = \frac{1}{2} \operatorname{erfc} \left[\left(\frac{2\sigma_5^2}{\mu_3^2} \right)^{-\frac{1}{2}} \right]. \quad (70)$$

Finally, the BER of the DCSK-DIM-II system in Case II is obtained as

$$P_{sys,II}^{(2)} = \psi(m_c, P_{map,II}^{(2)}, P_{mod,II}^{(2)}). \quad (71)$$

When the equiprobable transmitted information bits are considered, the overall bit error rate of DCSK-DIM-II system is stated as

$$P_{sys}^{(2)} = \frac{1}{P} P_{sys,I}^{(2)} + \frac{P-1}{P} P_{sys,II}^{(2)}. \quad (72)$$

Therefore, the average bit error probability of DCSK-DIM-II system over multipath Rayleigh fading channel can be expressed as

$$\bar{P}_{sys}^{(2)} = \int_0^\infty P_{sys}^{(2)} f(\gamma_s^{(2)}) d\gamma_s^{(2)}, \quad (73)$$

where $f(\gamma_s^{(2)})$ can be obtained in a similar manner of (44).

$$P_{ed,II}^{(2)} = \int_0^\infty \left\{ 1 - \left(\frac{1}{2} \right)^{P-2} \left[\operatorname{erfc} \left(\frac{\xi - \phi}{\sqrt{2\rho}} \right) + \operatorname{erfc} \left(\frac{\xi + \phi}{\sqrt{2\rho}} \right) \right]^{P-2} \left[\operatorname{erfc} \left(\frac{\xi - \phi}{\sqrt{2v}} \right) + \operatorname{erfc} \left(\frac{\xi + \phi}{\sqrt{2v}} \right) \right] \right\} \frac{2}{\sqrt{2\pi v}} e^{-\left(\frac{-\xi^2}{2v} \right)} d\xi. \quad (66)$$

V. NUMERICAL RESULTS AND DISCUSSIONS

In this section, the BER performances of the proposed DCSK-DIM-I and DCSK-DIM-II systems over AWGN and multipath Rayleigh fading channels are presented and discussed, verifying the superiority of the designs and the accuracy of our derivations. We employ the logistic map $x_{k+1} = 1 - x_k^2$, $k = 0, 1, 2, \dots$ to generate the chaotic signals in our simulation because of its simplicity and excellent statistic properties [29]. For brevity, unless otherwise stated, three paths Rayleigh fading channel with the equal average power gains $E(\alpha_1^2) = E(\alpha_2^2) = E(\alpha_3^2) = \frac{1}{3}$ are employed in simulations. Besides, for all multipath channel profiles, the delay spreads are varying according to $\tau_1=0$, $\tau_2 = 1$, $\tau_3 = 2$.

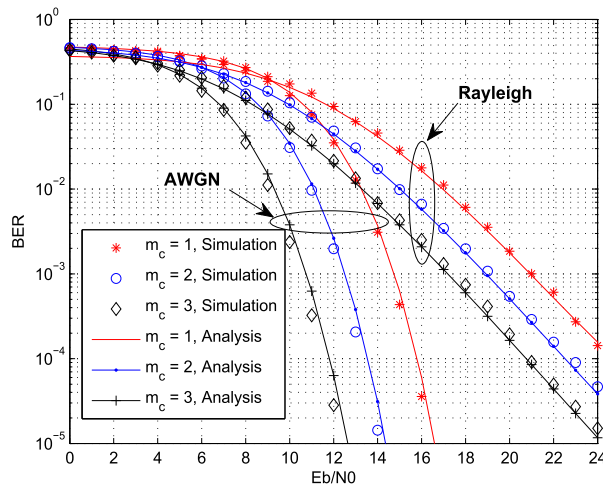


FIGURE 4. BER performance of DCSK-DIM-I system over AWGN and multipath Rayleigh fading channels with $\beta = 450$ and $m_c = 1, 2, 3$.

A. PERFORMANCE EVALUATION

In order to validate the former analysis, the simulation results of the proposed DCSK-DIM-I system are compared with the theoretical results over AWGN and multipath Rayleigh fading channels, as depicted in Fig. 4. Apparently, the figure shows the tight accordance between the simulation results and the analytical results, thus verifying the accuracy of our analysis approaches. Then, the numerical evaluation of BER performance also captures the behavior of the experimental data: the BER performance of the proposed DCSK-DIM-I system is deteriorating when the number of the mapped bits decreases. For instance, in AWGN channel, the required SNR of DCSK-DIM-I system must be approximately 4dB higher for $m_c = 1$ in contrast to $m_c = 3$ at a BER of 10^{-5} . This phenomenon can be explained that for larger m_c , more bits are mapped within a symbol for the same transmitted energy and the required SNR reduces. Furthermore, the BER performance of the DCSK-DIM-II system over AWGN and multipath Rayleigh fading channels are illustrated in Fig. 5. The simulation results almost match the corresponding theoretical results in the BER ranges of practical interest. On the

other hand, unlike the DCSK-DIM-I system, the proposed DCSK-DIM-II system delivers a similar BER performance in the cases of $m_c = 2$ and $m_c = 3$. The reason for the above difference lies in that the number of the active time slots of each branch is as many as $P - 1$ in DCSK-DIM-II system, which means there are great interference in index detection, leading to poor BER performance.

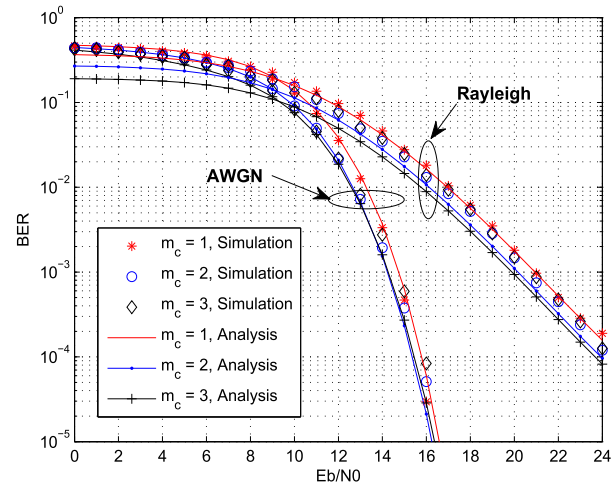


FIGURE 5. BER performance of DCSK-DIM-II system over AWGN and multipath Rayleigh fading channels with $\beta = 450$ and $m_c = 1, 2, 3$.

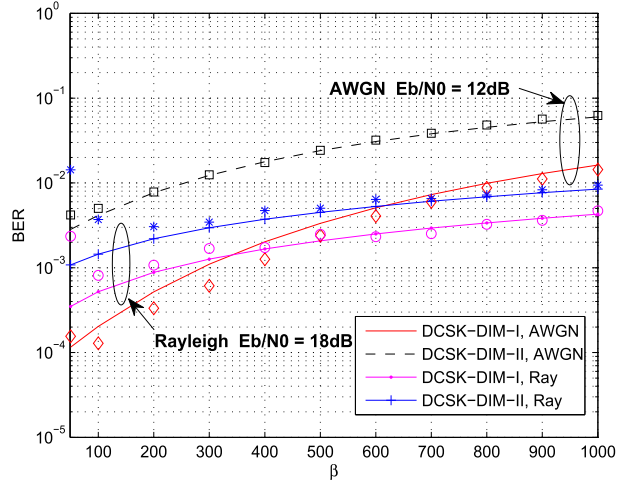


FIGURE 6. The influence of β on the BER performance over AWGN and multipath Rayleigh fading channels with $m_c = 2$. The lines represent the theoretical results and the markers denote simulation results.

Fig. 6 shows the effect of β on the BER performance of DCSK-DIM-I and DCSK-DIM-II systems over AWGN and multipath Rayleigh fading channels. Although the fitting degree is little disappointed when the spreading factor is small, there is a good agreement between the simulated and analytical results in high spreading factor, which further demonstrates that our analysis and derivation are valid and correct. In the case of AWGN channel, we observe that the BER performance of both DCSK-DIM-I and DCSK-DIM-II systems keep a deteriorating trend as the spreading factor increases, which is due to that more noise components will

be involved and thus result in more interference in index detection when the spreading factor enlarges. With respect to the case of multipath Rayleigh fading channel, when the spreading factor increases, the BER values of two systems above decline first, and then a climbing spreading factor leads to the deterioration of BER performance. To explain this phenomenon, we can elaborate that the multipath delay is ignored in our derivations of BER expressions and, however, the hypothesis of $0 < \tau_{\max} \ll \beta$, namely the multipath delay is far less than the symbol duration, is not satisfied in the simulations.

To illustrate the influence of inter symbol interference (ISI) on BER performance a little further, the performance of DCSK-DIM-I and DCSK-DIM-II systems are evaluated in two-path Rayleigh fading channel with the equal power gains, i.e., $E(\alpha_1^2) = E(\alpha_2^2) = \frac{1}{2}$ and different maximum multipath delay τ_{\max} . As clearly observed in Fig. 7, when the maximum multipath delay is rather lower, as expected, there is a perfect match between the simulation results and theoretical results which means the inter symbol interference can be neglected. However, with the increase of τ_{\max} , the inter symbol interference is dominant and can not be negligible. From another perspective, the BER performance of DCSK-DIM-II system is more susceptible to inter symbol interference in contrast to DCSK-DIM-I system which is owing to the fact that more time slots are active in DCSK-DIM-II system, leading to larger interference in index detection.

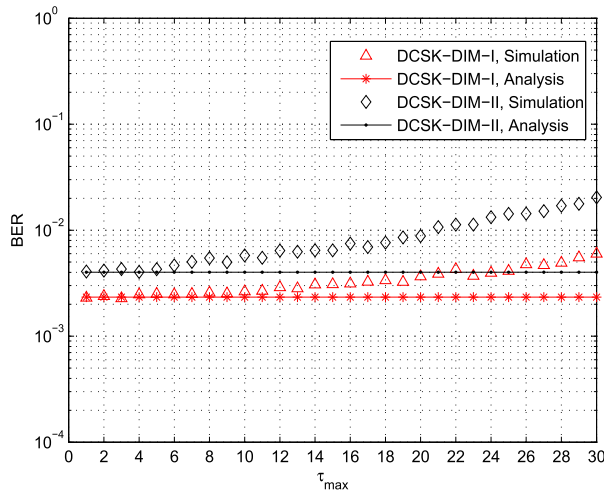


FIGURE 7. The influence of τ_{\max} on the BER performance of DCSK-DIM-I and DCSK-DIM-II systems over two-path Rayleigh fading channel with $E_b/N_0 = 20\text{dB}$, $\beta = 300$ and $m_c = 2$.

B. PERFORMANCE COMPARISON

As shown in Fig. 8, the BER performance of DCSK-DIM-I, DCSK-DIM-II and the recently proposed PPM-DCSK are compared over AWGN channel. Apparently, the proposed DCSK-DIM-I system can achieve the best BER performance compared to PPM-DCSK system under the same simulation parameters. For example, at a BER level of 10^{-4} , the performance of DCSK-DIM-I system is about 0.5dB better

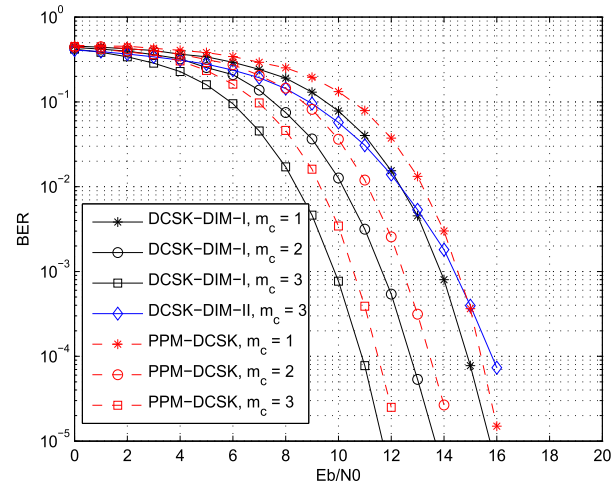


FIGURE 8. Performance comparisons between DCSK-DIM-I, DCSK-DIM-II and PPM-DCSK over AWGN channel with $\beta = 270$.

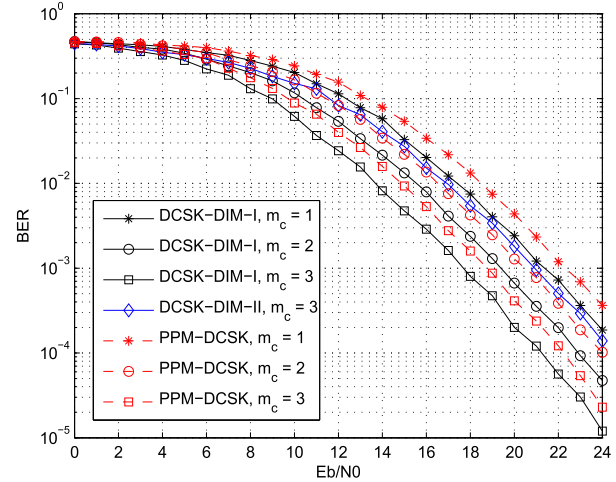


FIGURE 9. Performance comparisons between DCSK-DIM-I, DCSK-DIM-II and PPM-DCSK over multipath Rayleigh fading channel with $\beta = 540$.

than the counterpart of PPM-DCSK when $m_c = 3$. The recently proposed PPM-DCSK system shows a better BER performance than DCSK-DIM-II system when $m_c = 3$. Whereas, as displayed in Table 1, a welcome discovery appears that the data rate of DCSK-DIM-II system is five times that of PPM-DCSK system when $m_c = 3$. In other words, there is a trade-off between DCSK-DIM-II and the PPM-DCSK in terms of the data rate and BER performance. Moreover, we make a BER performance comparison between DCSK-DIM-I, DCSK-DIM-II and PPM-DCSK over multipath Rayleigh fading channel with $\beta = 540$. The outcome of this comparison is illustrated in Fig. 9. The results indicate that the proposed DCSK-DIM-I system shows rather robust in fading channel. In addition, as depicted in Table 1, the data rate of DCSK-DIM-I system is twice as much as that of PPM-DCSK system. Considering the demand of high data rate and the rugged environment of future wireless communication, the proposed DCSK-DIM-I system is up-and-coming.

Fig. 10 compares the BER performance of DCSK-DIM-I, DCSK-DIM-II and other non-coherent chaotic communication systems over AWGN and multipath Rayleigh

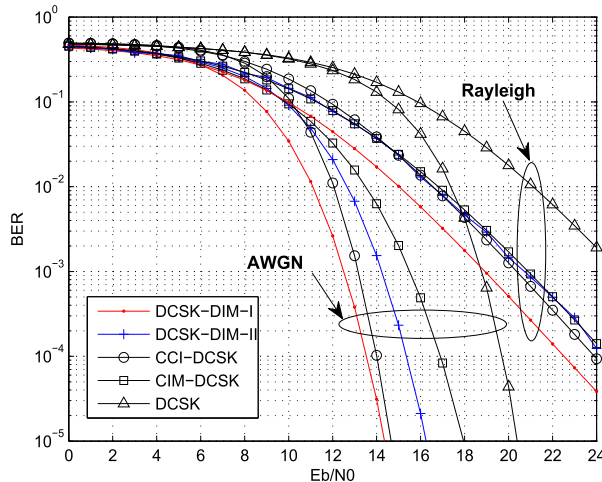


FIGURE 10. Performance comparisons between DCSK-DIM-I, DCSK-DIM-II and other non-coherent chaotic communication systems over AWGN and multipath Rayleigh fading channels with $\beta = 450$.

fading channels. For a relatively fair comparison, the number of overall bits per symbol is set to 6 (except for DCSK system) and there are 10 bits per symbol in DCSK-DIM-II system (Note that the DCSK-DIM-II system is the same as DCSK-DIM-I system when both systems possess 4 bits per transmitted symbol, thus the minimum number of transmitted bits per symbol in DCSK-DIM-II system is 10). Besides, $\beta = 450$ is applied for all system simulations. As clearly witnessed, to obtain the same BER performance, the required SNR of the proposed DCSK-DIM-I system is minimum. Explicitly, in the case of AWGN channel, CIM-DCSK system needs 18dB to reach the BER level of 10^{-5} , while the required SNR for the DCSK-DIM-I system is reduced to approximate 14dB at the same BER level above. As a result, the performance improvement between the DCSK-DIM-I system and CIM-DCSK system is about 4dB. It is worth noticing that although the BER performance of DCSK-DIM-I and CCI-DCSK systems are similar in AWGN channel, DCSK-DIM-I system performs much better than CCI-DCSK system in multipath Rayleigh fading channel, i.e., the BER performance gain of DCSK-DIM-I system over CCI-DCSK system is more than 1.5dB. The BER performance of DCSK-DIM-II system is inferior to the counterpart of CCI-DCSK system in AWGN channel. Nonetheless, the BER performance of DCSK-DIM-II system is quite close to that of CCI-DCSK system in multipath Rayleigh fading channel.

In Fig. 11, the comparisons of BER performance over AWGN and multipath Rayleigh fading channels are carried out among the DCSK-DIM-I, DCSK-DIM-II, CI-DCSK, 2CI-DCSK and PI-DCSK with $\beta = 128$. In general, the total transmitted bits per symbol is set to 6 in the above systems (apart from DCSK-DIM-II system) and 10 bits per symbol will be adopted in the DCSK-DIM-II system. Despite the BER performance of DCSK-DIM-I system is slightly worse than the counterpart of CI-DCSK system in the range of high SNR, apparently, opposite results appear in front of us when we take the low SNR into consideration. In the case of

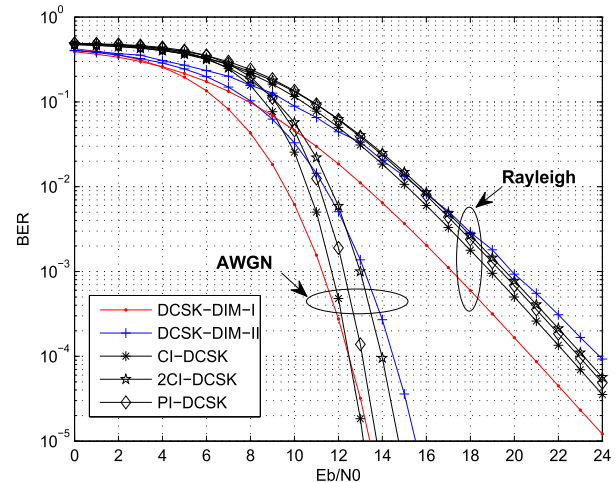


FIGURE 11. Performance comparisons between DCSK-DIM-I, DCSK-DIM-II and other non-coherent chaotic communication systems over AWGN and multipath Rayleigh fading channels with $\beta = 128$.

multipath Rayleigh fading channel, clearly, the BER performance improvement of DCSK-DIM-I system over CI-DCSK system is rather close to 2dB at 10^{-4} BER level. Therefore, it is worth noting that DCSK-DIM-I system exhibits admirable robustness to resist the degradation even in severe multipath environment. As a matter of fact, the performance improvement of the DCSK-DIM-I system is a consequence of dual-index modulation, i.e., more bits are mapped into the index symbols of in-phase and quadrature branches, reducing the required SNR to a great extent. Despite the dual-index modulation technique enables DCSK-DIM-II system to achieve preferable BER performance, the signals between different time slots brings huge interference to index detection and thus impede the performance improvement of DCSK-DIM-II system.

VI. CONCLUSION

In this paper, two promising differential chaos shift keying systems with dual-index modulation have been proposed and analyzed in an exhaustive manner. In the proposed systems, the overall transmitted bits are divided into the in-phase branch and quadrature branch, respectively, and then by means of dual-index modulation technique, the mapped bits of the in-phase and quadrature branches are modulated into a pair of distinguishable index symbols. Profiting from the dual-index modulation, the data rate, spectral efficiency and BER performance of the proposed DCSK-DIM systems are promoted significantly compared to the recently proposed PPM-DCSK system. Explicitly, the DCSK-DIM-I system makes a great progress in pursuit of admirable BER performance, while the DCSK-DIM-II system elevates the data rate to a great extent. In addition, the theoretical BER expressions of the proposed systems over AWGN and multipath Rayleigh fading channels have been derived at great length, and then the simulation results verify the accuracy of our derivations. In contrast to other non-coherent chaotic communication systems,

the proposed DCSK-DIM-I system can deliver preferable BER performance, while the DCSK-DIM-II system is more specifically suited for high throughput scenarios.

REFERENCES

- [1] Y. Xia, C. K. Tse, and F. C. M. Lau, "Performance of differential chaos-shift-keying digital communication systems over a multipath fading channel with delay spread," *IEEE Trans. Circuits Syst.-II*, vol. 51, no. 12, pp. 680–684, Dec. 2004.
- [2] J. Yu and Y.-D. Yao, "Detection performance of chaotic spreading LPI waveforms," *IEEE Trans. Wireless Commun.*, vol. 4, no. 2, pp. 390–396, Mar. 2005.
- [3] V. Lynnyk and S. Čelikovský, "On the anti-synchronization detection for the generalized Lorenz system and its applications to secure encryption," *Kybernetika*, vol. 46, no. 1, pp. 1–18, 2010.
- [4] H. Dedieu, M. P. Kennedy, and M. Hasler, "Chaos shift keying: Modulation and demodulation of a chaotic carrier using self-synchronizing Chua's circuits," *IEEE Trans. Circuits Syst. II, Analog Digit. Signal Process.*, vol. 40, no. 10, pp. 634–642, Oct. 1993.
- [5] L. M. Pecora and T. L. Carroll, "Synchronization in chaotic systems," *Phys. Rev. Lett.*, vol. 64, no. 8, pp. 821–824, 1990.
- [6] G. Kolumbán, M. P. Kennedy, and L. O. Chua, "The role of synchronization in digital communications using chaos. I. Fundamentals of digital communications," *IEEE Trans. Circuits Syst. I, Reg. Papers*, vol. 44, no. 10, pp. 927–936, Oct. 1997.
- [7] G. Kolumbán, M. P. Kennedy, and L. O. Chua, "The role of synchronization in digital communications using chaos. II. Chaotic modulation and chaotic synchronization," *IEEE Trans. Circuits Syst. I, Reg. Papers*, vol. 45, no. 11, pp. 1129–1140, Nov. 1998.
- [8] G. Kolumbán and M. P. Kennedy, "Communications using chaos/spl Gt/MINUS. III. Performance bounds for correlation receivers," *IEEE Trans. Circuits Syst. I, Reg. Papers*, vol. 47, no. 12, pp. 1673–1683, Dec. 2000.
- [9] G. Kolumbán, G. K. Vizvári, W. Schwarz, and A. Abel, "Differential chaos shift keying: A robust coding for chaos communication," in *Proc. NDES*. Seville, Spain, Jun. 1996, pp. 92–97.
- [10] F. C. M. Lau and C. K. Tse, *Chaos-Based Digital Communication Systems: Operating Principles, Analysis Methods, and Performance Evaluation*. Berlin, Germany: Springer, 2003.
- [11] Z. Galias and G. M. Maggio, "Quadrature chaos-shift keying: Theory and performance analysis," *IEEE Trans. Circuits Syst. I, Fundam. Theory Appl.*, vol. 48, no. 12, pp. 1510–1519, Dec. 2001.
- [12] L. Wang, G. Cai, and G. R. Chen, "Design and performance analysis of a new multiresolution M -ary differential chaos shift keying communication system," *IEEE Trans. Wireless Commun.*, vol. 14, no. 9, pp. 5197–5208, Sep. 2015.
- [13] G. Kis, "Performance analysis of chaotic communication systems," Ph.D. dissertation, Dept. Meas. Inf. Syst., Budapest Univ. Technol. Econ., Budapest, Hungary, 2005.
- [14] W. Xu, L. Wang, and G. Kolumbán, "A new data rate adaption communications scheme for code-shifted differential chaos shift keying modulation," *Int. J. Bifurcation Chaos*, vol. 22, no. 8, pp. 1–8, 2012.
- [15] T. Huang, L. Wang, W. Xu, and F. C. M. Lau, "Multilevel code-shifted differential-chaos-shift-keying system," *IET Commun.*, vol. 10, no. 10, pp. 1189–1195, Jul. 2016.
- [16] G. Kaddoum and F. Gagnon, "Design of a high-data-rate differential chaos-shift keying system," *IEEE Trans. Circuits Syst.-II*, vol. 59, no. 7, pp. 448–452, Jul. 2012.
- [17] X. Cai, W. Xu, R. Zhang, and L. Wang, "A multilevel code shifted differential chaos shift keying system with M -ary modulation," *IEEE Trans. Circuits Syst. II, Exp. Briefs*, to be published. doi: [10.1109/TCSIL.2018.2886377](https://doi.org/10.1109/TCSIL.2018.2886377).
- [18] G. Kaddoum and E. Soujiri, "On the comparison between code-index modulation and spatial modulation techniques," in *Proc. Int. Conf. Inf. Commun. Technol. Res.(ICTRC)*. Abu Dhabi, UAE, May 2015, pp. 24–27.
- [19] E. Basar, M. Wen, R. Mesleh, M. Di Renzo, Y. Xiao, and H. Haas, "Index modulation techniques for next-generation wireless networks," *IEEE Access*, vol. 5, pp. 16693–16746, 2017.
- [20] G. Kaddoum, M. F. A. Ahmed, and Y. Nijsure, "Code index modulation: A high data rate and energy efficient communication system," *IEEE Commun. Lett.*, vol. 19, no. 2, pp. 175–178, Feb. 2015.
- [21] G. Kaddoum, Y. Nijsure, and T. Hung, "Generalized code index modulation technique for high-data-rate communication systems," *IEEE Trans. Veh. Technol.*, vol. 65, no. 9, pp. 7000–7009, Sep. 2016.
- [22] W. Xu, T. Huang, and L. Wang, "Code-shifted differential chaos shift keying with code index modulation for high data rate transmission," *IEEE Trans. Commun.*, vol. 65, no. 10, pp. 4285–4294, Oct. 2017.
- [23] Y. Tan, W. Xu, T. Huang, and L. Wang, "A multilevel code shifted differential chaos shift keying scheme with code index modulation," *IEEE Trans. Circuits Syst. II, Express Briefs*, vol. 65, no. 11, pp. 1743–1747, Nov. 2018.
- [24] G. Kaddoum, E. Soujiri, and Y. Nijsure, "Design of a short reference non-coherent chaos-based communication systems," *IEEE Trans. Commun.*, vol. 64, no. 2, pp. 680–689, Jan. 2016.
- [25] W. Xu, Y. Tan, F. C. M. Lau, and G. Kolumbán, "Design and optimization of differential chaos shift keying scheme with code index modulation," *IEEE Trans. Commun.*, vol. 66, no. 5, pp. 1970–1980, May 2018.
- [26] G. Kaddoum and E. Soujiri, "NR-DCSK: A noise reduction differential chaos shift keying system," *IEEE Trans. Circuits Syst. II, Exp. Briefs*, vol. 63, no. 7, pp. 648–652, Jul. 2016.
- [27] W. Xu and L. Wang, "Performance optimization for short reference differential chaos shift keying scheme," in *Proc. IEEE Int. Conf. Signal Process., Commun. Comput. (ICSPCC)*, Oct. 2017, pp. 1–6.
- [28] M. Herceg, D. Vranješ, G. Kaddoum, and E. Soujiri, "Commutation code index DCSK modulation technique for high-data-rate communication systems," *IEEE Trans. Circuits Syst. II, Express Briefs*, vol. 65, no. 12, pp. 1954–1958, Dec. 2018.
- [29] M. Herceg, G. Kaddoum, D. Vranješ, and E. Soujiri, "Permutation index DCSK modulation technique for secure multiuser high-data-rate communication systems," *IEEE Trans. Veh. Technol.*, vol. 67, no. 4, pp. 2997–3011, Apr. 2018.
- [30] G. Kaddoum, F. Richardson, and F. Gagnon, "Design and analysis of a multi-carrier differential chaos shift keying communication system," *IEEE Trans. Commun.*, vol. 61, no. 8, pp. 3281–3291, Aug. 2013.
- [31] G. Cheng, L. Wang, W. Xu, and G. Chen, "Carrier index differential chaos shift keying modulation," *IEEE Trans. Circuits Syst. II, Exp. Briefs*, vol. 64, no. 8, pp. 907–911, Aug. 2017.
- [32] G. Cheng, L. Wang, Q. Chen, and G. Chen, "Design and performance analysis of generalised carrier index M -ary differential chaos shift keying modulation," *IET Commun.*, vol. 12, no. 11, pp. 1324–1331, Jul. 2018.
- [33] W. Dai, H. Yang, Y. Song, and G. Jiang, "Two-layer carrier index modulation scheme based on differential chaos shift keying," *IEEE Access*, vol. 6, pp. 56433–56444, 2018.
- [34] M. Miao, L. Wang, M. Katz, and W. Xu, "Hybrid modulation scheme combining PPM with differential chaos shift keying modulation," *IEEE Wireless Commun. Lett.*, to be published. doi: [10.1109/LWC.2018.2871137](https://doi.org/10.1109/LWC.2018.2871137).
- [35] A. Papoulis, *Probability, Random Variables, and Stochastic Processes*. New York, NY, USA: McGraw-Hill, 1991.
- [36] J. G. Proakis and M. Salehi, *Digital Communications*. New York, NY, USA: McGraw-Hill, 2007.



XIANGMING CAI received the B.Sc. degree in information engineering from the Guangdong University of Technology, Guangzhou, China, in 2017. He is currently pursuing the M.Sc. degree with the Department of Information and Communication Engineering, Xiamen University, Fujian, China. His research interest includes chaos-based digital communications and their applications to wireless communications.



WEIKAI XU (S'10–M'12) received the B.S. degree in electronic engineering from Three Gorges College, Chongqing, China, in 2000, the M.Sc. degree in communication and information system from the Chongqing University of Posts and Telecommunications, Chongqing, China, in 2003, and the Ph.D. degree in electronic circuit and system from the Xiamen University of China, Xiamen, China, in 2011. From 2003 to 2012, he was a Teaching Assistant and an Assistant Professor in communication engineering with Xiamen University, where he is currently an Associate Professor in information and communication engineering. His research interests include chaotic communications, underwater acoustic communications, channel coding, cooperative communications, and ultra-wideband.

Professor in communication engineering with Xiamen University, where he is currently an Associate Professor in information and communication engineering. His research interests include chaotic communications, underwater acoustic communications, channel coding, cooperative communications, and ultra-wideband.



FANG XU received the B.S. degree in electric automation from the Shandong University of Science and Technology, Shandong, China, in 1994, the M.Sc. degree in signal and information processing from the Chongqing University of Posts and Telecommunications, Chongqing, China, in 1997, and the Ph.D. degree in communication and information systems from Xiamen University, Xiamen, China, in 2010.

From 1997 to 2013, she was an Assistant Professor and an Associate Professor with the Communication Engineering Department, Xiamen University, where she is currently a Senior Engineer with the National Information Experimental Teaching Center for Electronic Information. Her research interests include multicarrier modulation, cooperative communications, and underwater acoustic communications.

• • •



LIN WANG (S'99–M'03–SM'09) received the M.Sc. degree in applied mathematics from the Kunming University of Technology, China, in 1988, and the Ph.D. degree in electronics engineering from the University of Electronic Science and Technology of China, China, in 2001. From 1984 to 1986, he was a Teaching Assistant with the Mathematics Department, Chongqing Normal University. From 1989 to 2002, he was a Teaching Assistant, a Lecturer, and an Associate

Professor in applied mathematics and communication engineering with the Chongqing University of Posts and Telecommunication, China. From 1995 to 1996, he was with the Mathematics Department, University of New England, Armidale, NSW, Australia, for one year. In 2003, he was a Visiting Researcher with the Center for Chaos and Complexity Networks, Department of Electronic Engineering, City University of Hong Kong, for three months. In 2013, he was a Senior Visiting Researcher with the Department of ECE, University of California at Davis, Davis, CA, USA. From 2003 to 2012, he was a Full Professor and an Associate Dean with the School of Information Science and Engineering, Xiamen University, China, where he has been a Distinguished Professor since 2012. He holds 14 patents in physical layer in digital communications. He has authored more than 100 journal and conference papers. His current research interests include channel coding, joint source and channel coding, chaos modulation, and their applications to wireless communication, and storage systems.